Supporting Information

Electronegativity-Driven d-Band Center Shifts in Ru-Ni Alloys for Low Methane Hydrogenolysis of Polyolefin Plastics

*Qianfeng Zhou[1a], Huijie Li[1a], Shengdong Zhang[a], Changhu Leng[a], Chuanya Li[a], Yongchao Wang[a], Chenyang Ma[a], Wanglei Wang[a], Xiaogang Fu[a], Lei Zhu[b,c], Tengshijie Gao[b,c], Cheng Wang[b,c], Li-Zhu Wu[*b,c], Zhi-Jun Li[*a]*

[a] State Key Laboratory of Solidification Processing, Atomic Control & Catalysis Engineering Laboratory (ACCEL), School of Materials Science and Engineering, Northwestern Polytechnical University, Xi'an, Shaanxi 710072, P.R. China

[b] Key Laboratory of Photochemical Conversion and Optoelectronic Materials, Technical Institute of Physics and Chemistry & University of Chinese Academy of Sciences, Chinese Academy of Sciences, Beijing 100190, P. R. China

[c] School of Future Technology, University of Chinese Academy of Sciences, Beijing 100049, P.R. China

* Corresponding author.

E-mail addresses: zhijunli@nwpu.edu.cn **(Zhi-Jun Li),** lzwu@mail.ipc.ac.cn **(Li-Zhu Wu)**

[1] Qianfeng Zhou and Huijie Li contributed equally to this work.

Figures

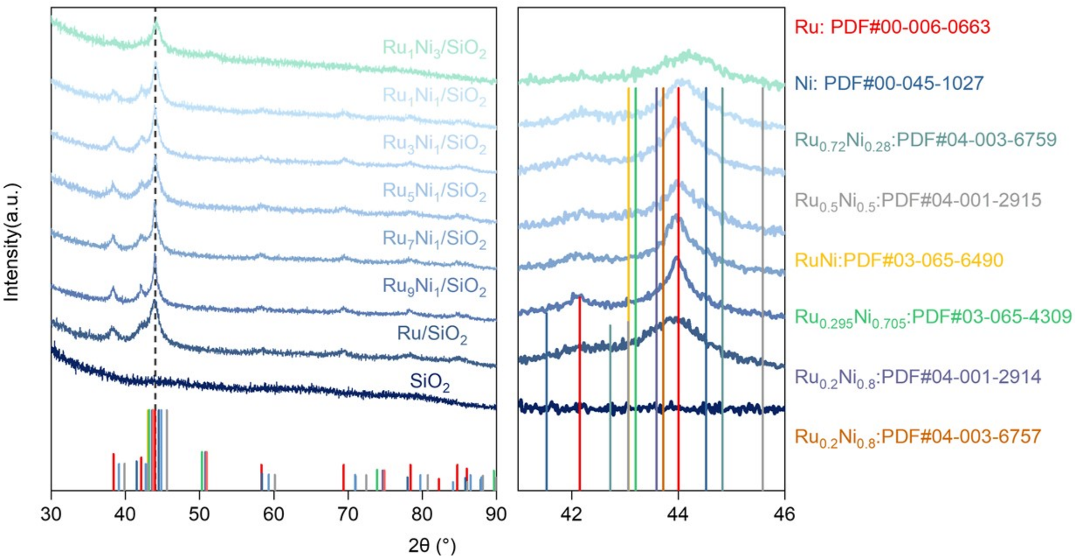

Figure S1 XRD patterns of mono-metallic Ru/SiO_2 and bi-metallic Ru_xNi_y/SiO_2 catalysts. The XRD patterns show a shift to higher angles as the Ni content increases, indicating successful alloying of Ni with Ru[1].

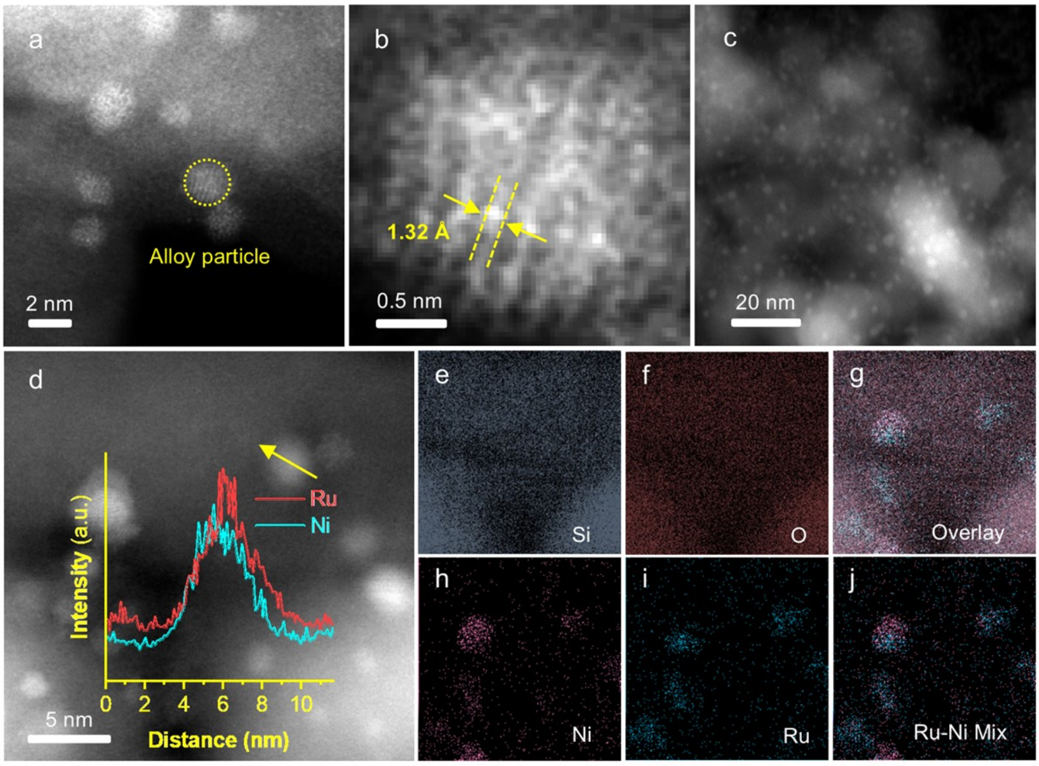

Figure S2 (a-d) HAADF-STEM images and (e-j) EDS mapping of the Ru_1Ni_3/SiO_2 catalyst.

The metal NPs formed by the Ru_1Ni_3/SiO_2 catalyst have an average diameter of 2-5 nm. EDS mapping and line-scanning show the co-localized distribution of Ru and Ni, confirming the formation of a Ru-Ni bimetallic alloy[2]. Lattice fringes with an interplanar distance of 1.32 Å, corresponding to the (110) planes of Ru in the alloy NPs, were observed. This distance is shorter than the 1.35 Å interplanar distance of Ru (110) crystal faces, further supporting the formation of bimetallic Ru-Ni alloy NPs.

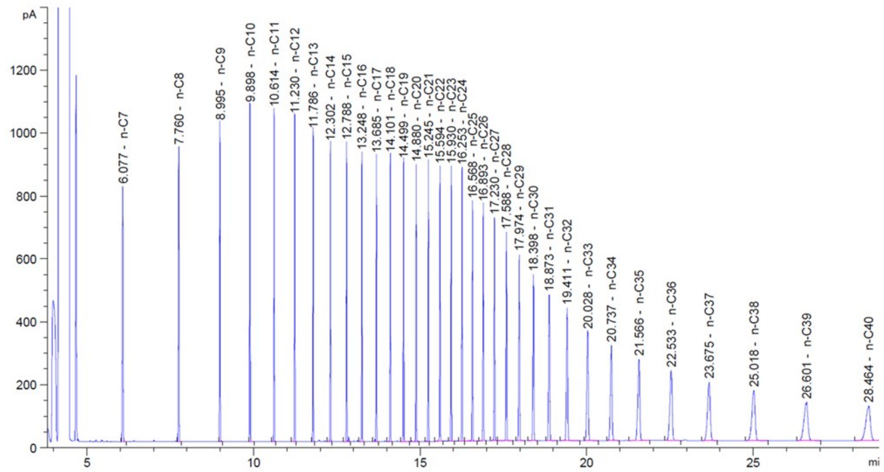

Figure S3 GC-FID analysis of standard alkane reference materials (C7-C40, 1 mg·mL^{-1} in n-hexane).

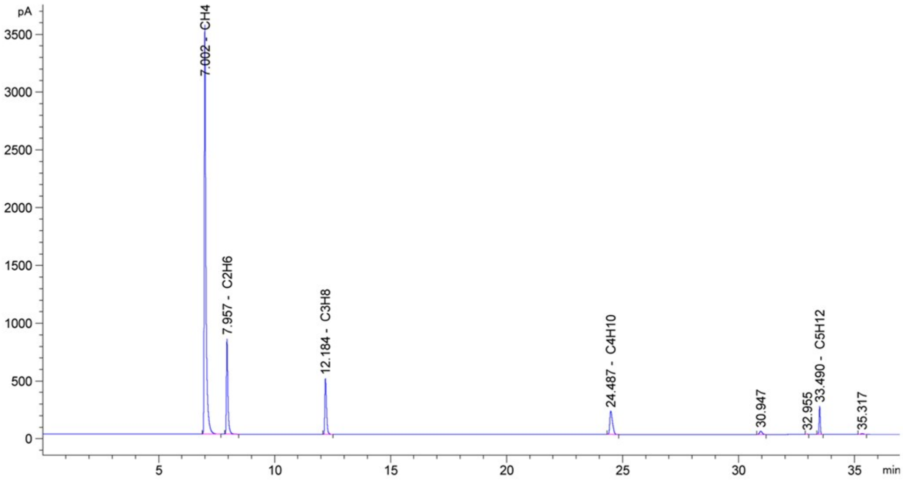

Figure S4 Typical GC-FID analysis of gas products obtained from HDPE. Reaction conditions: 1 g HDPE (M_w = 40.3 kDa), 250 °C, 12 h, 3 MPa H_2, 50 mg Ru_3Ni_1/SiO_2.

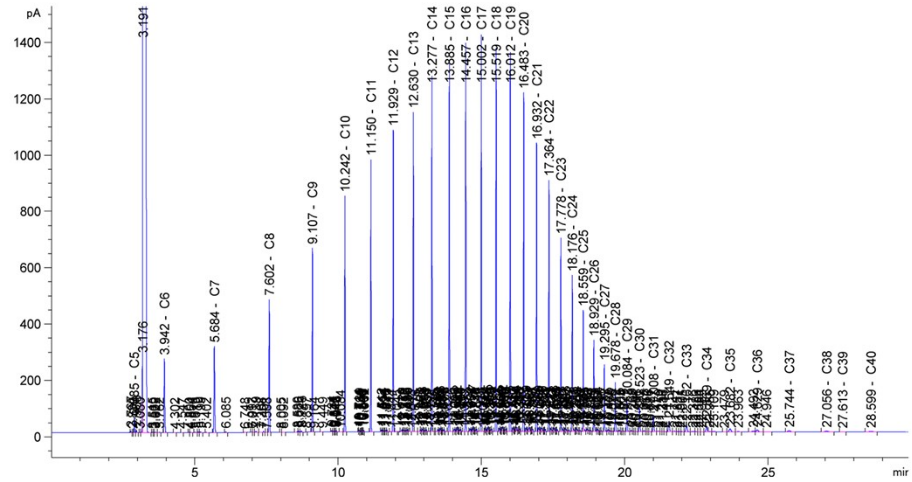

Figure S5 Typical GC-FID analysis of liquid products obtained from HDPE. Reaction conditions: 1 g HDPE (M_w = 40.3 kDa), 250 °C, 12 h, 3 MPa H_2, 50 mg Ru_3Ni_1/SiO_2. Comparison with the retention times of linear alkanes from Figure S3 shows that most of the products are linear alkanes, with a narrow, bell-shaped distribution.

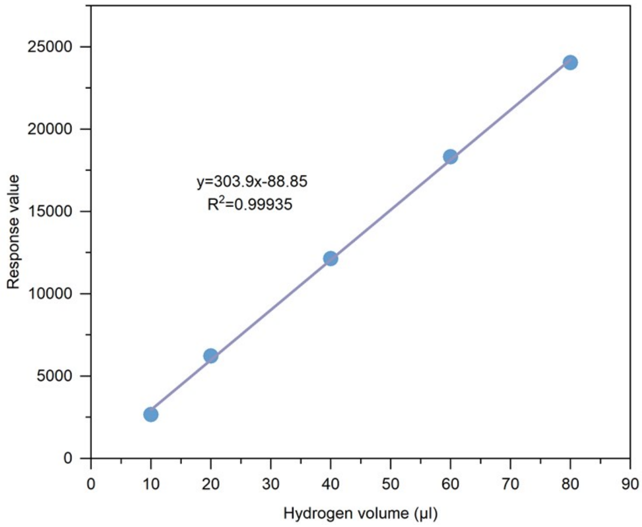

Figure S6 The standard curve between hydrogen volume and the TCD response value.

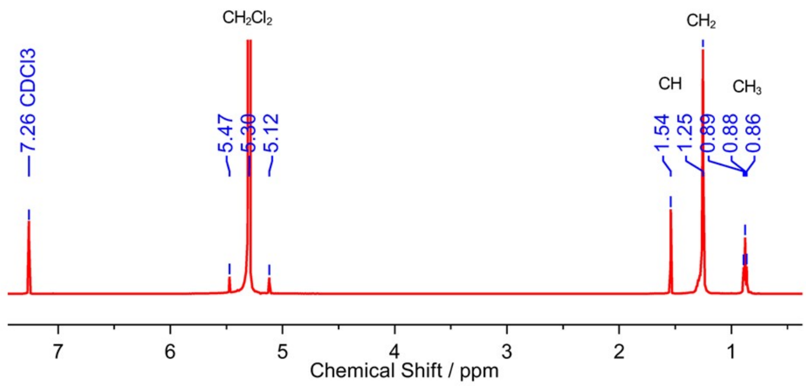

Figure S7 ^{1}H-NMR spectrum of liquid products from HDPE hydrogenolysis. Reaction conditions: 250 °C, 3 MPa H_2, 1 g HDPE, 50 mg Ru_3Ni_1/SiO_2, 12 h.

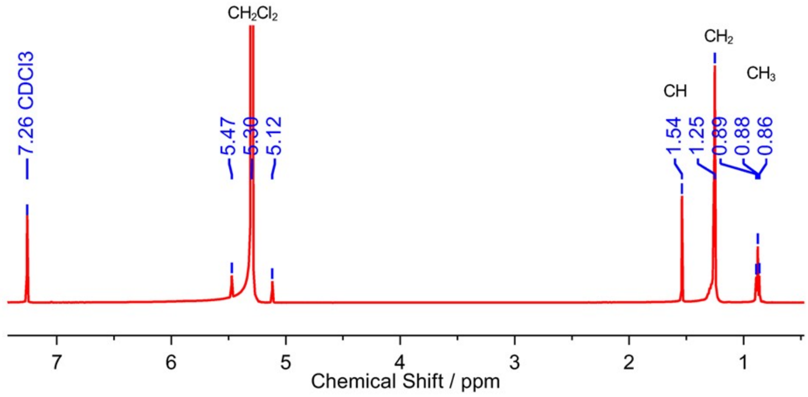

Figure S8 ^{1}H-NMR spectrum of liquid products from HDPE hydrogenolysis. Reaction conditions: 250 °C, 3 MPa H_2, 1 g HDPE, 100 mg Ru_1Ni_3/SiO_2, 36 h.

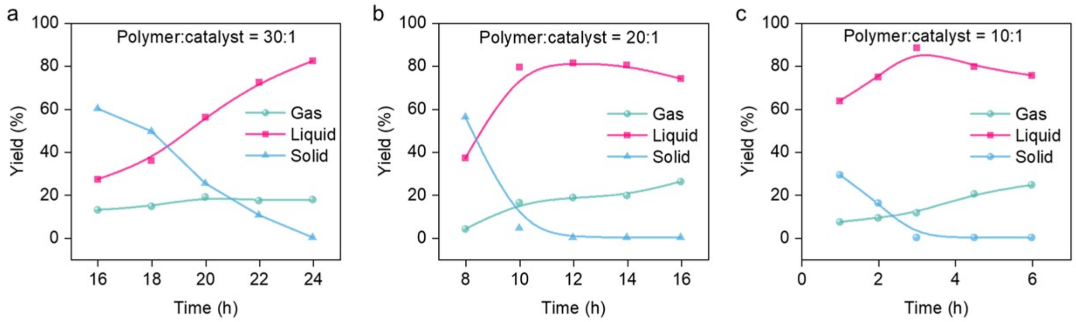

Figure S9 (a-c) Effect of feed ratio on catalytic performance of Ru_3Ni_1/SiO_2 catalysts. Reaction conditions: 250 °C, 3 MPa H_2, 1 g HDPE, 50 mg Ru_3Ni_1/SiO_2.

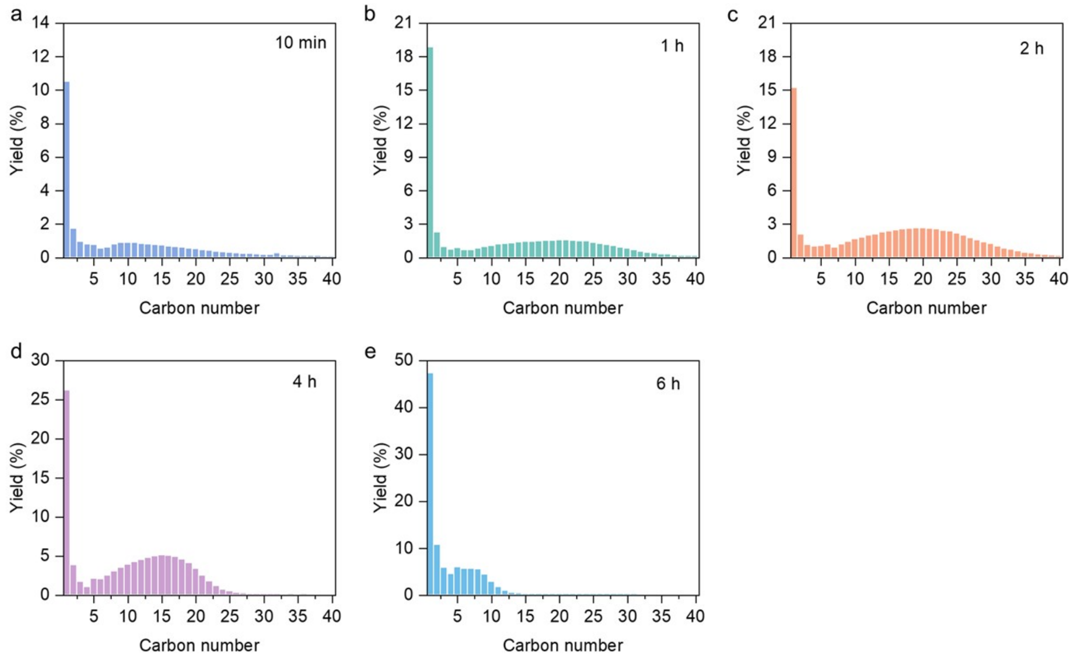

Figure S10 Hydrogenolysis products of HDPE with Ru/SiO_2 over time. (a) 10 min, (b) 1 h, (c) 2 h, (d) 4 h, and (e) 6 h. Reaction conditions: 250 °C, 3 MPa H_2, 1 g HDPE, 50 mg catalyst. Ru/SiO_2 and Ru_3Ni_1/SiO_2 have the same Ru loading.

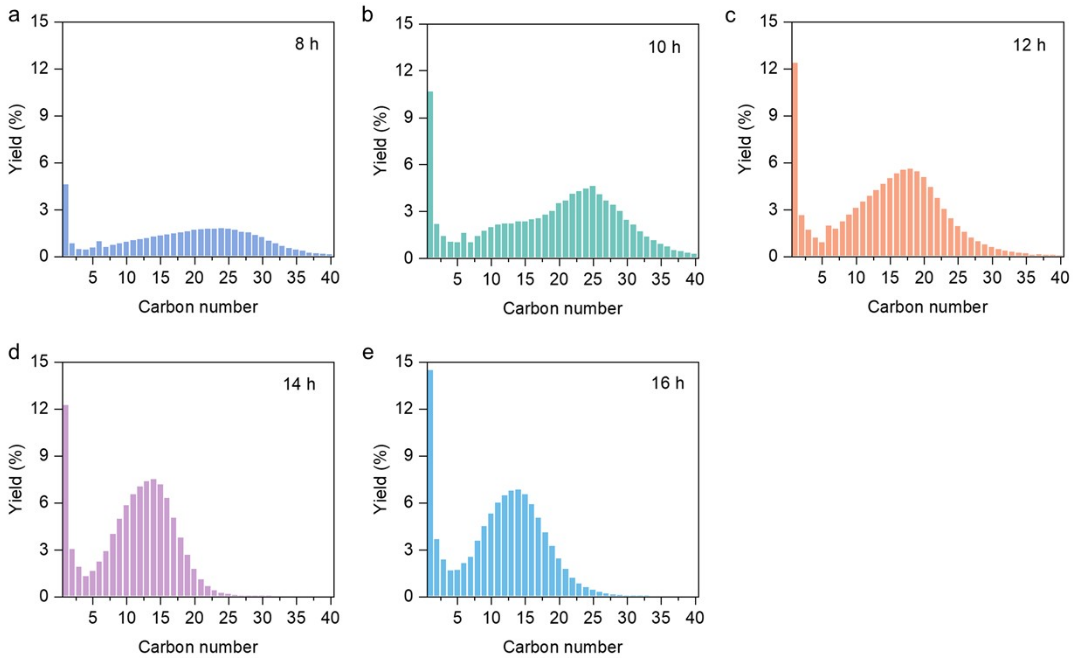

Figure S11 Hydrogenolysis products of HDPE with Ru_3Ni_1/SiO_2 over time. (a) 8 h, (b) 10 h, (c) 12 h, (d) 14 h, and (e) 16 h. Reaction conditions: 250 °C, 3 MPa H_2, 1 g HDPE, 50 mg catalyst.

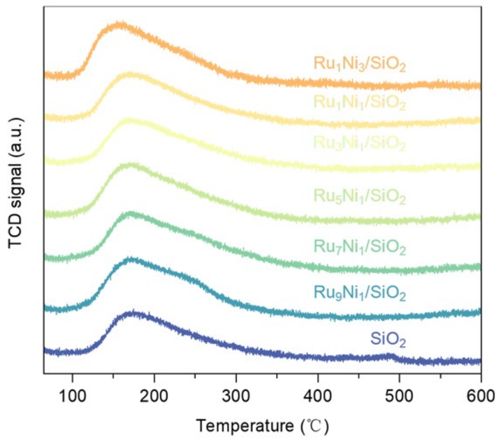

Figure S12 NH_3-TPD profiles of SiO_2 and Ru-Ni bimetallic catalysts.

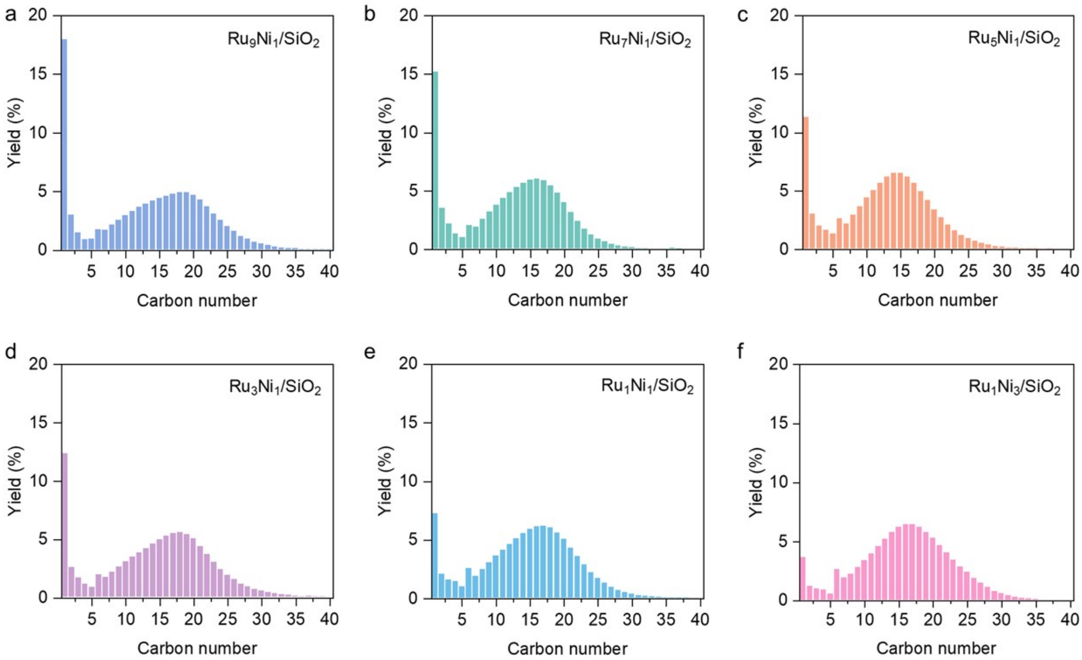

Figure S13 HDPE hydrogenolysis product distribution for Ru_xNi_y/SiO_2 catalysts. (a) 250 °C, 3 MPa H_2, 1 g HDPE, 50 mg Ru_9Ni_1/SiO_2, 6 h; (b) 250 °C, 3 MPa H_2, 1 g HDPE, 50 mg Ru_7Ni_1/SiO_2, 6 h; (c) 250 °C, 3 MPa H_2, 1 g HDPE, 50 mg Ru_5Ni_1/SiO_2, 12 h; (d) 250 °C, 3 MPa H_2, 1 g HDPE, 50 mg Ru_3Ni_1/SiO_2, 12 h; (e) 250 °C, 3 MPa H_2, 1 g HDPE, 100 mg Ru_1Ni_1/SiO_2, 18 h; (f) 250 °C, 3 MPa H_2, 1 g HDPE, 100 mg Ru_1Ni_3/SiO_2, 36 h.

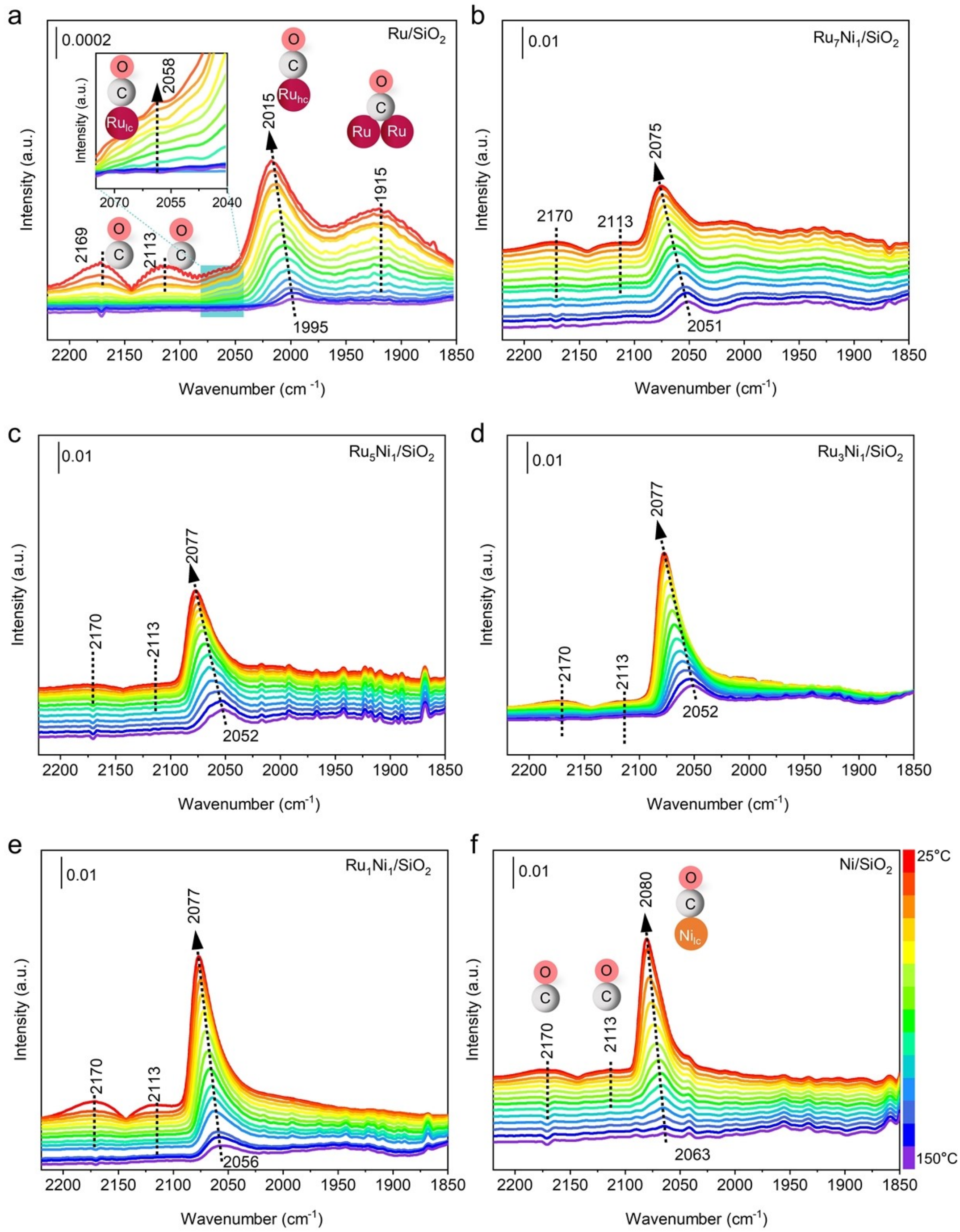

Figure S14 In situ CO-DRIFTS spectra of Ru_xNi_y/SiO_2 of (a) Ru/SiO_2 (b) Ru_7Ni_1/SiO_2 (c) Ru_5Ni_1/SiO_2 (d) Ru_3Ni_1/SiO_2 (e) $Ru1Ni_1/SiO_2$ (f) N_i/SiO_2 within 2250-1850 cm^{-1} by flowing N_2 gas.

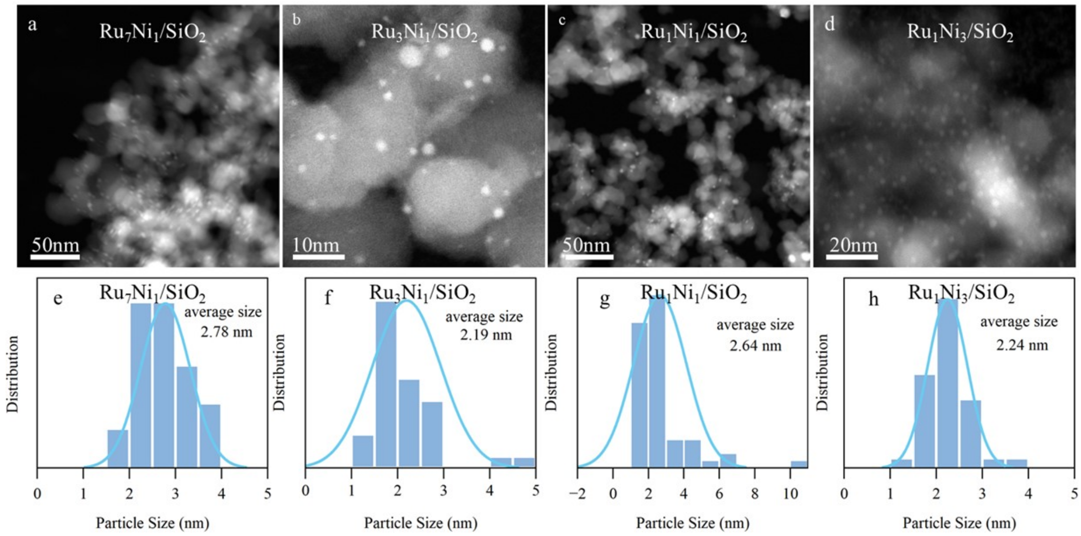

Figure S15 The HAADF images (a-d) and particle size distribution (e-h) of the Ru_7Ni_1/SiO_2, Ru_3Ni_1/SiO_2, Ru_1Ni_1/SiO_2, and Ru_1Ni_3/SiO_2 catalyst.

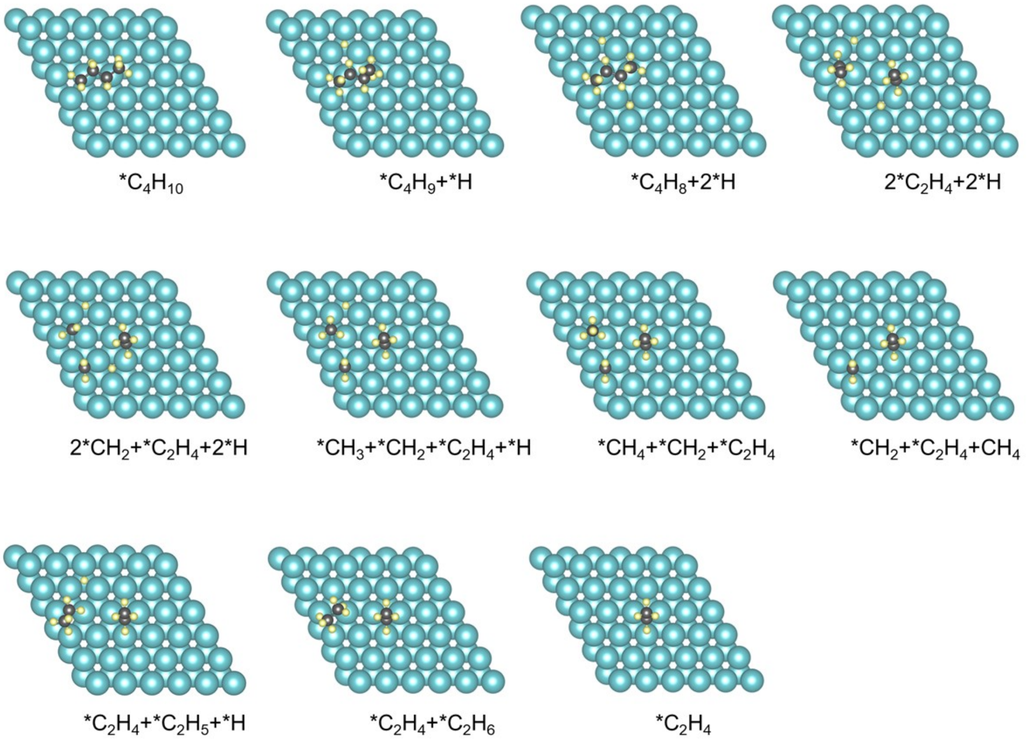

Figure S16 Adsorption configurations of intermediates on the Ru (0001) surface. In the atomic model, Ru atoms are represented in olive-green, C in black, and H in yellow.

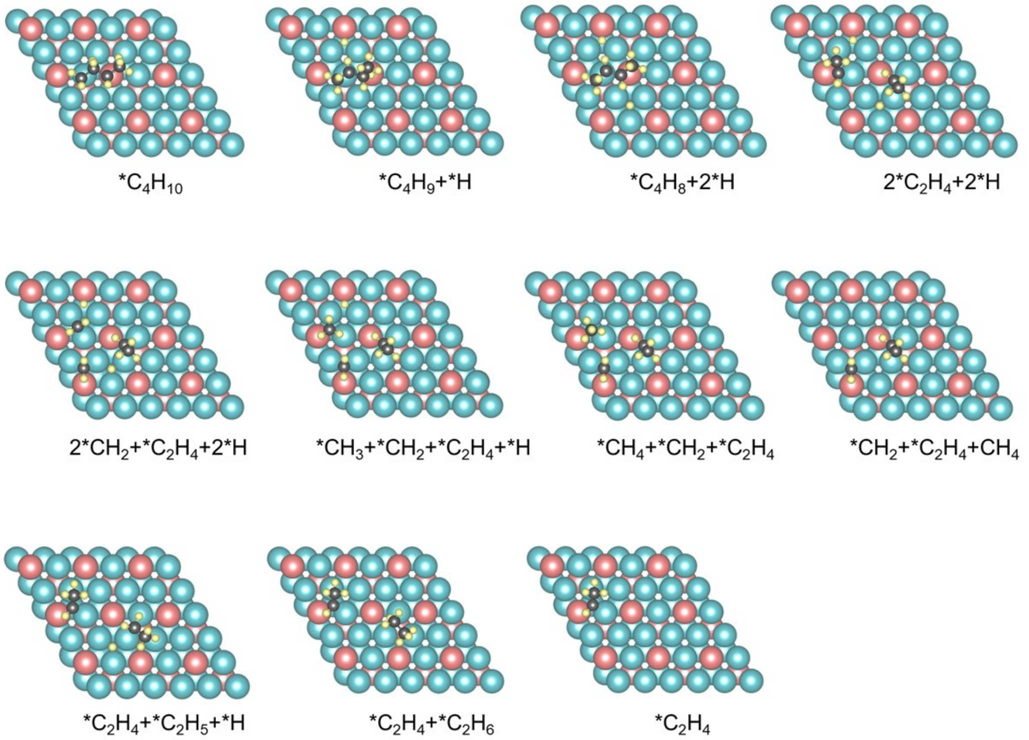

Figure S17 Adsorption configurations of intermediates on the Ru_3Ni_1 (0001) surface. In the atomic model, Ru atoms are represented in olive-green, Ni in light red, C in black, and H in yellow.

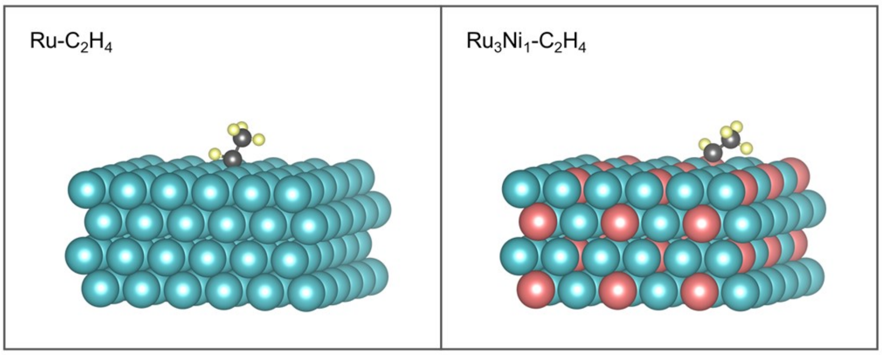

Figure S18 Adsorption configurations of *C_2H_4 on Ru (0001) and Ru_3Ni_1(0001) surfaces. In the atomic model, Ru atoms are represented in olive-green, Ni in light red, C in black, and H in yellow.

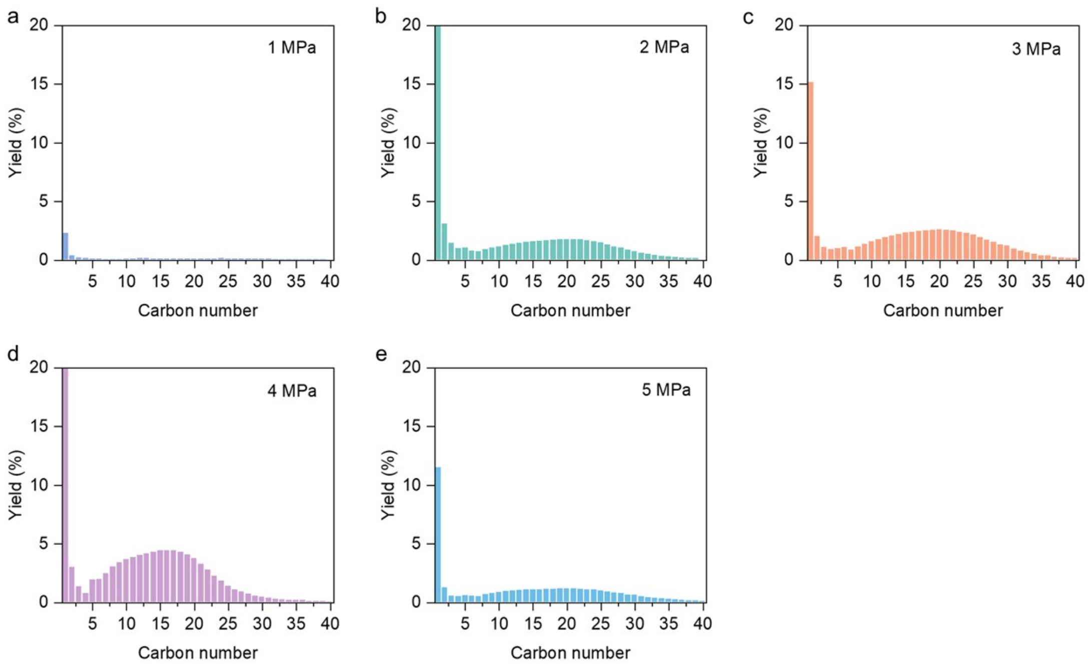

Figure S19 Hydrogenolysis products of HDPE with Ru/SiO_2 at varying H_2 pressures. (a-e) Reaction conditions: 250 °C, 1 g HDPE, 50 mg catalyst, 2 h.

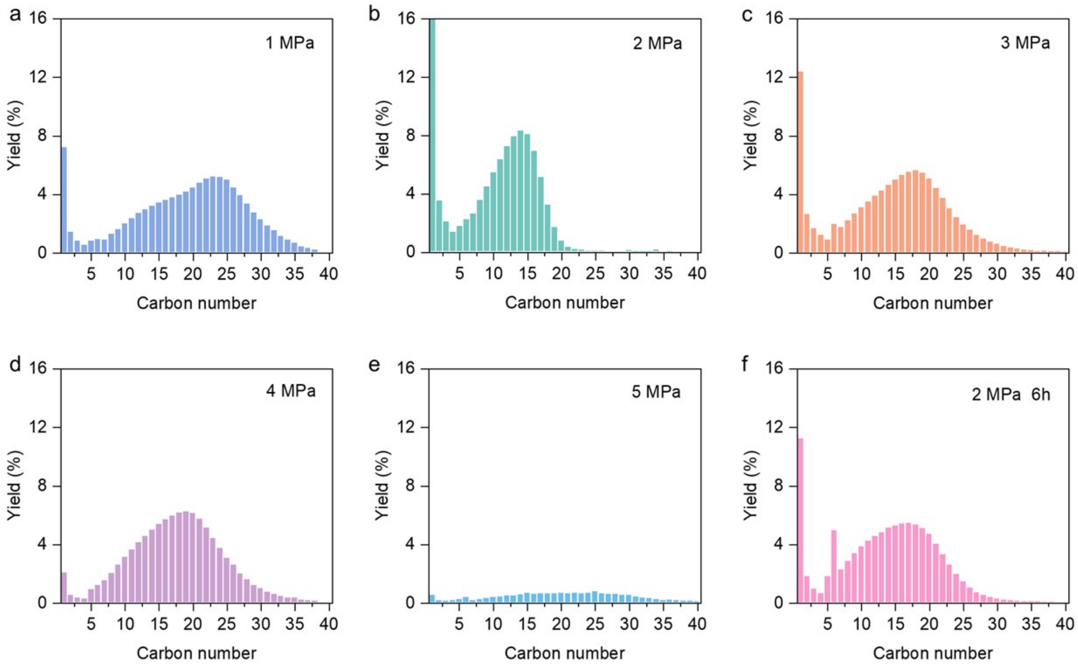

Figure S20 Hydrogenolysis products of HDPE with Ru_3Ni_1/SiO_2 at varying H_2 pressures. (a-e) Reaction conditions: 250 °C, 1 g HDPE, 50 mg catalyst, 12 h, 1-5 MPa. (f) Hydrogenolysis products of HDPE with Ru_3Ni_1/SiO_2 at 250 °C, 1 g HDPE, 50 mg catalyst, 6 h, 2 MPa.

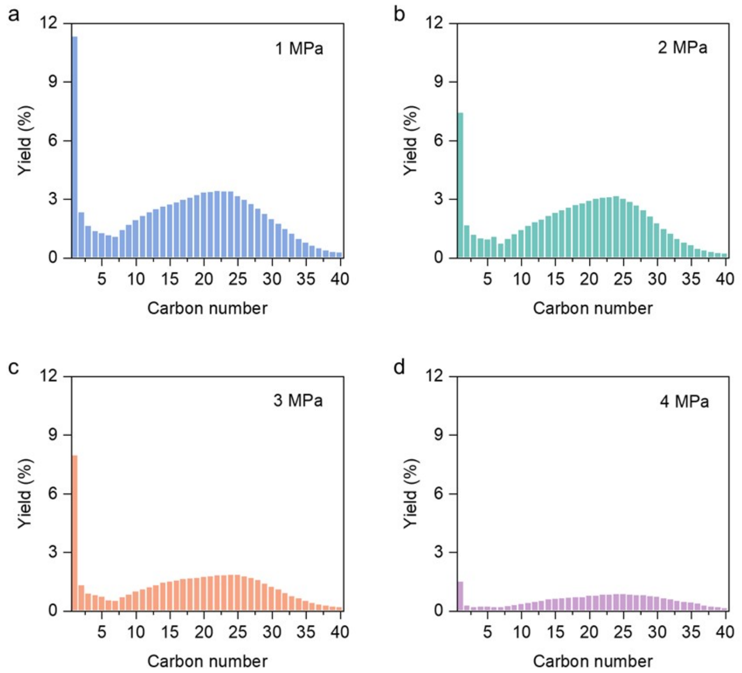

Figure S21 Hydrogenolysis products of HDPE with Ru_1Ni_3/SiO_2 at varying H_2 pressures. (a-d) Reaction conditions: 250 °C, 1 g HDPE, 100 mg catalyst, 24 h.

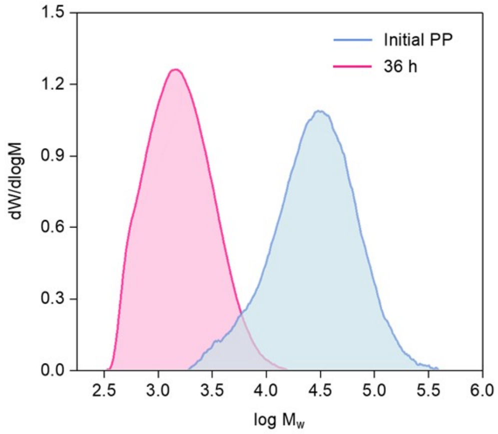

Figure S22 GPC analysis of molecular mass and distribution of initial PP and PP after hydrogenolysis using Ru_3Ni_1/SiO_2. The distribution is expressed as dW/d (log M), where dW is the weight fraction of eluted polymer and M is the molecular weight. Reaction conditions: 250 °C, 3 MPa H_2, 1 g PP (M_w = 40.2 kDa), 100 mg Ru_3Ni_1/SiO_2, 36 h.

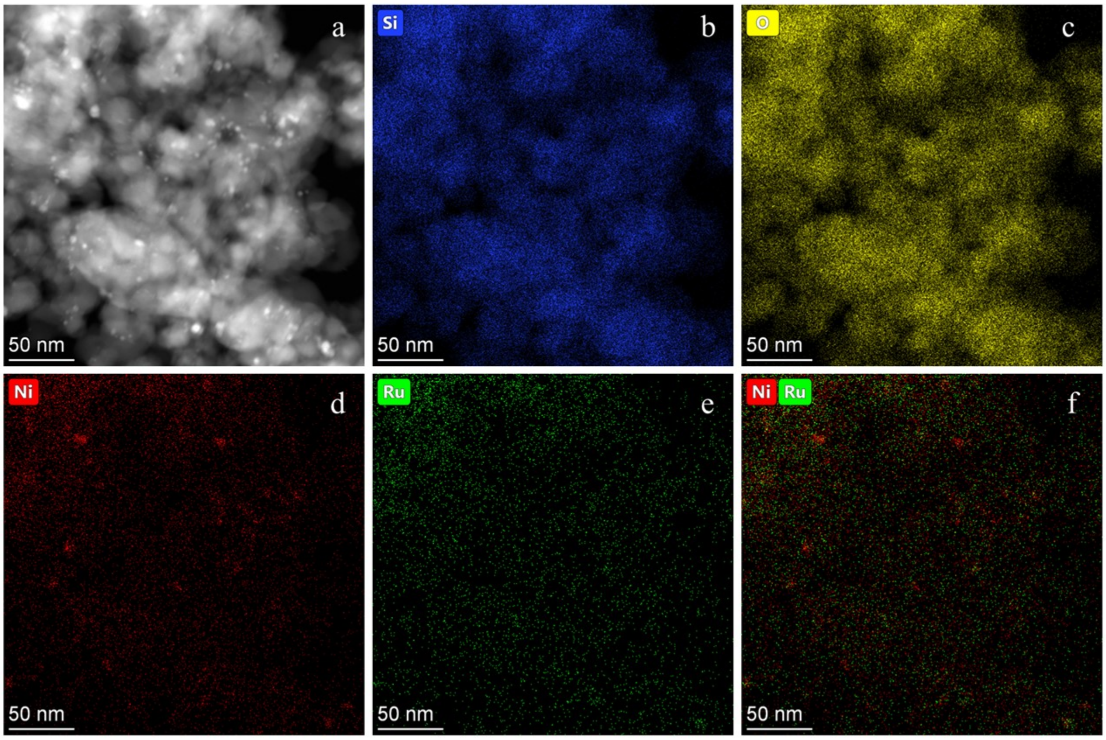

Figure S23 TEM images of the spent Ru_3Ni_1/SiO_2 catalyst.

TEM analysis revealed uniform dispersion of Ru and Ni, with the formed alloy particles maintaining a consistent size distribution (2–5 nm)—comparable to the fresh catalyst—indicating no significant particle aggregation during the reaction.

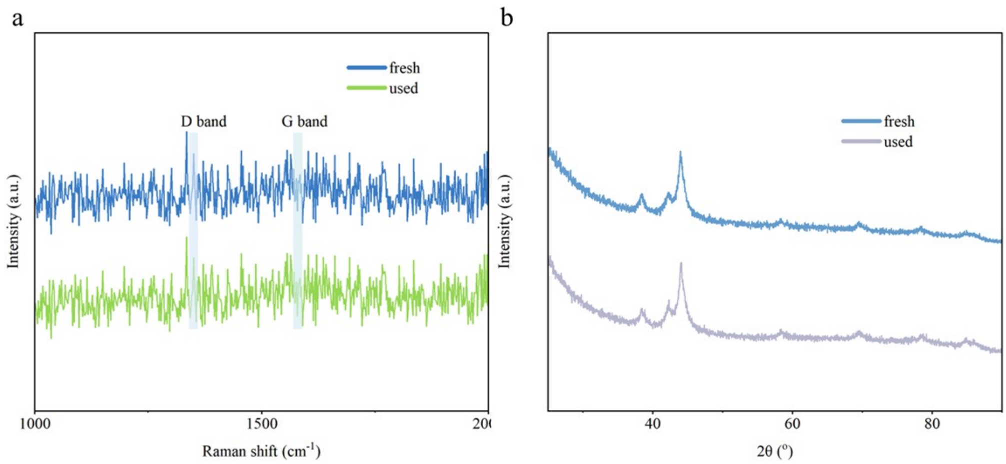

Figure S24 Raman spectra and XRD for fresh and used Ru_3Ni_1/SiO_2 catalyst.

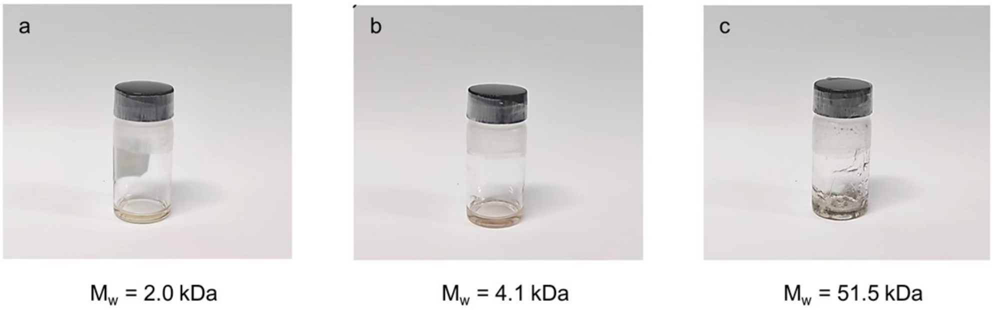

Figure S25 High-viscosity lubricants obtained by hydrogenolysis of PP. (a) 250 °C, 3 MPa H_2, 1 g PP (M_w = 40.2 kDa), 100 mg Ru_3Ni_1/SiO_2, 36 h; (b) 250 °C, 3 MPa H_2, 1 g plastic cup, 100 mg Ru_3Ni_1/SiO_2, 21 h; (c) 250 °C, 3 MPa H_2, 1 g plastic lids, 100 mg Ru_3Ni_1/SiO_2, 24 h.

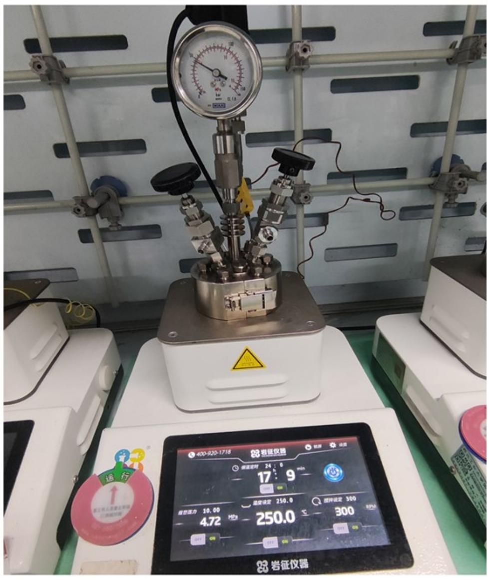

Figure S26 High-temperature and high-pressure reactor used for polyolefin hydrogenolysis reactions (Shanghai Yanzheng Experimental Instrument Co., Ltd.).

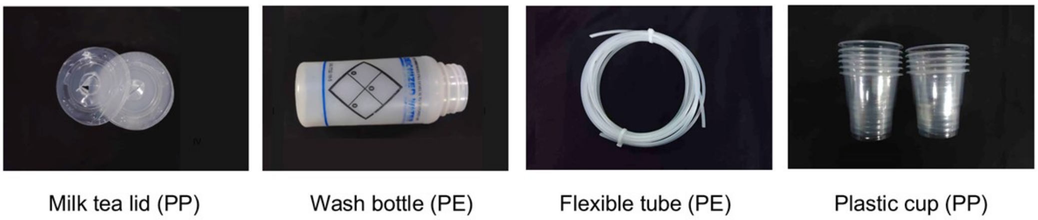

Figure S27 Commercial plastics used in hydrogenolysis. These post-consumer plastic wastes were simply washed, dried, and ground into powders with a particle size of approximately 100–500 mesh before being directly fed into the reactor for reaction.

Tables

Table S1 ICP-OES results for bi-metallic Ru_xNi_y/SiO_2 catalysts.

Catalysts	Ru loading	Ni loading	Ru/Ni atom ratio
Ru_1Ni_3/SiO_2	2.03	2.41	0.48
Ru_3Ni_1/SiO_2	2.92	0.55	3.08
Ru_7Ni_1/SiO_2	3.65	0.28	7.66

Table S2 H_2-TPR results for Ru/SiO_2, Ni/SiO_2 and Ru_3Ni_1/SiO_2 catalysts.

Catalysts	H_2 consumption (μmol/g)
Ru/SiO_2	536.11
Ni/SiO_2	284.26
Ru_3Ni_1/SiO_2	807.54

Table S3 Ru_3Ni_1/SiO_2 Catalyst Ru 3p Orbitals XPS Fitting Parameters.

Orbit	Peak	Height	Area	FWHM (eV)
Ru $3p_{3/2}$	461.2	282.75	1031.18	3.50
Ru $3p_{3/2}$	464.5	124.49	454.01	3.50
Ru $3p_{1/2}$	484.0	139.6	509.13	3.50
Ru $3p_{1/2}$	487.8	59.79	218.06	3.50

Table S4 Ru/SiO_2 Catalyst Ru 3p Orbitals XPS Fitting Parameters.

Orbit	Peak	Height	Area	FWHM (eV)
Ru $3p_{3/2}$	461.5	325.54	1187.24	3.50
Ru $3p_{3/2}$	464.7	113.09	553.99	3.50
Ru $3p_{1/2}$	484.1	185.55	676.7	3.50
Ru $3p_{1/2}$	487.2	84.28	307.35	3.50

Table S5 Reaction conditions for HDPE (M_w = 40.3 kDa) hydrogenolysis with SiO_2, Ni/SiO_2, Ru/SiO_2, Ru/SiO_2 + Ni/SiO_2 mechanical mixtures, and Ru_3Ni_1/SiO_2 catalysts.

Catalysts	**Polymer catalyst mass ratio**	**Initial Hydrogen Pressure (MPa)**	**Reaction temperature (°C)**	**Reaction time (h)**	**Conversion (wt%)**	**C_5-C_{40} Yield (wt%)**
SiO_2	20	3	250	12	1.97	0.77
Ni/SiO_2	20	3	250	12	3.12	2.08
Ru/SiO_2	20	3	250	12	100	10.05
Ru/SiO_2 + Ni/SiO_2	10	3	250	12	100	6.2
Ru_3Ni_1/SiO_2	20	3	250	12	100	82.2

Table S6 Effect of temperature on hydrogenolysis reactions with Ru_3Ni_1/SiO_2 catalysts.

Catalysts	Polymer/ catalyst mass ratio	Initial Hydrogen Pressure (MPa)	Reaction temperature (℃)	Reaction time (h)	Conversion (wt%)	C_5-C_{40}Yield (wt%)
Ru_3Ni_1/SiO_2	30	3	250	24	100	82.3
Ru_3Ni_1/SiO_2	20	3	250	12	100	82.2
Ru_3Ni_1/SiO_2	10	3	250	3	100	88.5
Ru_3Ni_1/SiO_2	20	3	225	48	48.8	42.2
Ru_3Ni_1/SiO_2	10	3	225	24	100	89.3

Table S7 NH_3-TPD results for bi-metallic Ru_xNi_y/SiO_2 catalysts.

Catalysts	**NH_3 adsorbed (μmol/g)**
SiO_2	112.26
Ru_9Ni_1/SiO_2	143.64
Ru_7Ni_1/SiO_2	131.37
Ru_5Ni_1/SiO_2	142.60
Ru_3Ni_1/SiO_2	122.39
Ru_1Ni_1/SiO_2	124.64
Ru_1Ni_3/SiO_2	137.88

Table S8 Effect of the Ru/Ni atomic ratio on catalyst activity and product selectivity.

Catalysts	Polymer catalyst mass ratio	Hydrogen Pressure (MPa)	Reaction temperature (℃)	Reaction time (h)	Conversion (wt%)	C_5-C_{40} Yield (wt%)	X_{H2}
Ru_9Ni_1/SiO_2	20	3	250	6	100	76.7	34.0
Ru_7Ni_1/SiO_2	20	3	250	6	100	77.8	24.2
Ru_5Ni_1/SiO_2	20	3	250	12	100	82.1	19.9
Ru_3Ni_1/SiO_2	20	3	250	12	100	82.2	19.0
Ru_1Ni_1/SiO_2	10	3	250	18	100	87.7	17.3
Ru_1Ni_3/SiO_2	10	3	250	36	100	93.3	12.8

Table S9 Effect of H_2 pressure on hydrogenolysis reactions with Ru/SiO_2 catalysts.

Catalysts	**Polymer catalyst mass ratio**	**Initial Hydrogen Pressure (MPa)**	**Reaction temperature (℃)**	**Reaction time (h)**	**Conversion (wt%)**	**C_5-C_{40} Yield (wt%)**
Ru/SiO_2	20	1	250	2	5.3	2.5
Ru/SiO_2	20	2	250	2	63.3	36.6
Ru/SiO_2	20	3	250	2	71.9	52.8
Ru/SiO_2	20	4	250	2	100	74.4
Ru/SiO_2	20	5	250	2	39.6	25.9

Table S10 Effect of H_2 pressure on hydrogenolysis reactions with Ru_3Ni_1/SiO_2 catalysts.

Catalysts	**Polymer catalyst mass ratio**	**Initial Hydrogen Pressure (MPa)**	**Reaction temperature (℃)**	**Reaction time (h)**	**Conversion (wt%)**	**C_5-C_{40} Yield (wt%)**
Ru_3Ni_1/SiO_2	20	1	250	12	100	90.2
Ru_3Ni_1/SiO_2	20	2	250	12	100	76.4
Ru_3Ni_1/SiO_2	20	3	250	12	100	82.2
Ru_3Ni_1/SiO_2	20	4	250	12	100	96.9
Ru_3Ni_1/SiO_2	20	5	250	12	16.1	15.2
Ru_3Ni_1/SiO_2	20	2	250	6	100	85.5

Table S11 Effect of H_2 pressure on hydrogenolysis reactions with Ru_1Ni_3/SiO_2 catalysts.

Catalysts	**Polymer catalyst mass ratio**	**Initial Hydrogen Pressure (MPa)**	**Reaction temperature (℃)**	**Reaction time (h)**	**Conversion (wt%)**	**C_5-C_{40}Yield (wt%)**
Ru_1Ni_3/SiO_2	10	1	250	24	89.1	72.5
Ru_1Ni_3/SiO_2	10	2	250	24	73.5	62.3
Ru_1Ni_3/SiO_2	10	3	250	24	50.7	39.8
Ru_1Ni_3/SiO_2	10	4	250	24	20.2	18.2
Ru_1Ni_3/SiO_2	10	5	250	24	0	0

Table S12 Hydrogenolysis performance of different plastics.

Catalysts	Plastics	M_w	Polymer catalyst mass ratio	Initial Hydrogen Pressure (MPa)	Reaction time (h)	Conversion (wt%)	Liquid yield (wt%)
Ru_3Ni_1/SiO_2	LDPE	61.9 kDa	20	3	16	100	73.6
Ru_3Ni_1/SiO_2	LLDPE	23.9 kDa	20	3	8	100	88.3
Ru_3Ni_1/SiO_2	HDPE	40.3 kDa	20	3	12	100	82.2
Ru_3Ni_1/SiO_2	PP	40.2 kDa	10	3	36	100	87.0

Table S13 Hydrogenolysis performance of various post-consumer plastics.

Catalysts	Polymer catalyst mass ratio	Plastics	Initial Hydrogen Pressure (MPa)	Reaction temperature (°C)	Reaction time (h)	Conversion (wt%)	Liquid yield (wt%)
Ru_3Ni_1/SiO_2	10	Milk tea lid (PP)	3	250	24	96.6	91.9
Ru_3Ni_1/SiO_2	20	Wash Bottle (PE)	3	250	12	100	61.9
Ru_3Ni_1/SiO_2	20	Flexible tube (PE)	3	250	14	100	63.0
Ru_3Ni_1/SiO_2	10	Plastic cup (PP)	3	250	21	99.7	88.0

Table S14 Comparison of Ru_3Ni_1/SiO_2 with literature catalysts for the catalytic hydrogenolysis of polyolefin plastics.

Catalysts	Initial Hydrogen Pressure (MPa)	Reaction temperature (°C)	Reaction time (h)	Gas selectivity (wt%)	Reference
Ru/C	2	200	16	50	[3]
Ru/TiO_2	3	250	20	31	[4]
Ru/CeO_2-5%	3.5	240	10	12.9	[5]
Ru/WZr	5	250	2	16	[6]
Ru/CeO_2-0.125%	3	260	18	33	[7]
Ru/ZrO_2	3.5	240	10	13.9	[8]
Ru/CeO_2-0.2%-SAC	2	250	6	7.5	[9]
Ru/TiO_2-A-SG	3	260	18	22	[10]
P-Ru-SBA	2	230	5	10	[11]
Ru@NTO-NH	4	240	18	13	[12]
Ru/C-EG120	2	240	1.5	13	[13]
$RuPt/ZrO_2$	3	240	8	10.5	[14]
Ru_9Pt_{91}/C	0.5	300	12	3	[15]
Ru_3Ni_1/SiO_2	4	250	12	3	**this work**
Ru_3Ni_1/SiO_2	1	250	12	9.8	**this work**

References

1. A. K. Manal, G. V. Shanbhag and R. Srivastava, *Appl. Catal. B-Environ.*, 2023, **338**, 123021.
2. Y. Dong, Q. Sun, C. Zhan, J. Zhang, H. Yang, T. Cheng, Y. Xu, Z. Hu, C.-W. Pao, H. Geng and X. Huang, *Adv. Funct. Mater.*, 2023, **33**, 2210328.
3. Julie E. Rorrer, Gregg T. Beckham and Y. Román-Leshkov, *JACS Au*, 2021, **1**, 8-12.
4. P. A. Kots, S. Liu, B. C. Vance, C. Wang, J. D. Sheehan and D. G. Vlachos, *ACS Catal.*, 2021, **11**, 8104-8115.
5. Y. Nakaji, M. Tamura, S. Miyaoka, S. Kumagai, M. Tanji, Y. Nakagawa, T. Yoshioka and K. Tomishige, *Appl. Catal. B-Environ.*, 2021, **285**, 119805.
6. C. Wang, T. Xie, P. A. Kots, B. C. Vance, K. Yu, P. Kumar, J. Fu, S. Liu, G. Tsilomelekis, E. A. Stach, W. Zheng and D. G. Vlachos, *JACS Au*, 2021, **1**, 1422-1434.
7. L. Chen, L. C. Meyer, L. Kovarik, D. Meira, X. I. Pereira-Hernandez, H. Shi, K. Khivantsev, O. Y. Gutiérrez and J. Szanyi, *ACS Catal.*, 2022, **12**, 4618-4627.
8. M. Tamura, S. Miyaoka, Y. Nakaji, M. Tanji, S. Kumagai, Y. Nakagawa, T. Yoshioka and K. Tomishige, *Appl. Catal. B-Environ.*, 2022, **318**, 121870.
9. M. Chu, X. Wang, X. Wang, X. Lou, C. Zhang, M. Cao, L. Wang, Y. Li, S. Liu, T.-K. Sham, Q. Zhang and J. Chen, *Research*, 2023, **6**, 0032.
10. L. Chen, J. B. Moreira, L. C. Meyer and J. Szanyi, *Appl. Catal. B-Environ.*, 2023, **335**, 122897.
11. Q. Kang, M. Chu, P. Xu, X. Wang, S. Wang, M. Cao, O. Ivasenko, T.-K. Sham, Q. Zhang, Q. Sun and J. Chen, *Angew. Chem. Int. Ed.*, 2023, **62**, e202313174.
12. X. Zhang, Q. Gan, P. Zhou, Z. Chen, Z. Zhang and G.-P. Lu, *Appl. Catal. B-Environ.*, 2024, **344**, 123626.
13. P. Hu, C. Zhang, M. Chu, X. Wang, L. Wang, Y. Li, T. Yan, L. Zhang, Z. Ding, M. Cao, P. Xu, Y. Li, Y. Cui, Q. Zhang, J. Chen and L. Chi, *J. Am. Chem. Soc.*, 2024, **146**, 7076-7087.
14. C. Sun, J. Wang, J. Wang, M. Shakouri, B. Shi, X. Liu, Y. Guo, Y. Hu, X.-P. Wu and Y. Wang, *Appl. Catal. B-Environ.*, 2024, **353**, 124046.
15. Q. Hu, S. Qian, Y. Wang, J. Zhao, M. Jiang, M. Sun, H. Huang, T. Gan, J. Ma, J. Zhang, Y. Cheng and Z. Niu, *Nat. Commun.*, 2024, **15**, 10573.

.